Biochimica et Biophysica Acta 1838 (2014) 3025–3035

Contents lists available at ScienceDirect

Biochimica et Biophysica Acta

journal homepage: www.elsevier.com/locate/bbamem

Biochemical characterization and structure–function relationship of two plant NCS2 proteins, the nucleobase transporters NAT3 and NAT12 from *Arabidopsis thaliana*

Sandra Niopek-Witz [a], Johannes Deppe [a], M. Joanne Lemieux [b], Torsten Möhlmann [a,*]

[a] Pflanzenphysiologie, Fachbereich Biologie, Universität Kaiserslautern, Erwin-Schrödinger-Straße, D-67663 Kaiserslautern, Germany
[b] Membrane Protein Disease Research Group, Department of Biochemistry, University of Alberta, Edmonton, Alberta, Canada

ARTICLE INFO

Article history:
Received 2 June 2014
Received in revised form 30 July 2014
Accepted 9 August 2014
Available online 16 August 2014

Keywords:
NCS2
Nucleobase ascorbate transporter
Homology model
Mutagenesis
Arabidopsis thaliana
Uracil

ABSTRACT

Nucleobase ascorbate transporters (NATs), also known as Nucleobase:Cation-Symporter 2 (NCS2) proteins, belong to an evolutionary widespread family of transport proteins with members in nearly all domains of life. We present the biochemical characterization of two NAT proteins, NAT3 and NAT12 from *Arabidopsis thaliana* after their heterologous expression in *Escherichia coli* UraA knockout mutants. Both proteins were shown to transport adenine, guanine and uracil with high affinities. The apparent K_M values were determined with 10.12 μM, 4.85 μM and 19.95 μM, respectively for NAT3 and 1.74 μM, 2.44 μM and 29.83 μM, respectively for NAT12. Competition studies with the three substrates suggest hypoxanthine as a further substrate of both transporters. Furthermore, the transport of nucleobases was markedly inhibited by low concentrations of a proton uncoupler indicating that NAT3 and NAT12 act as proton–nucleobase symporters. Transient expression studies of NAT-GFP fusion constructs revealed a localization of both proteins in the plasma membrane. Based on the structural information of the uracil permease UraA from *E. coli*, a three-dimensional experimentally validated homology model of NAT12 was created. The NAT12 structural model is composed of 14 TM segments and divided into two inverted repeats of TM1–7 and TM8–14. Docking studies and mutational analyses identified residues involved in NAT12 nucleobase binding including Ser-247, Phe-248, Asp-461, Thr-507 and Thr-508. This is the first study to provide insight into the structure–function of plant NAT proteins, which reveals differences from the other members of the NCS2 protein family.

1. Introduction

Nucleobase transport systems can be found in almost all domains of life. In prokaryotes like *Escherichia coli* (*E. coli*) nucleobase transport proteins belong to the nucleobase cation symporter NCS1 and NCS2 families [34]. While their expression is widespread, key differences are found for these two distantly related transporter families.

NCS1 proteins, also known as purine related transporters generally transport purines as proton symporters and can be found in archaea, bacteria, yeast, fungi and plants [34]. *E. coli* NCS1 proteins are CodB [9], a cytosine specific transporter and YbbW, a putative nucleobase transporter [8]. In *Arabidopsis*, the plastidic nucleobase transporter PLUTO represents the only NCS1 member and was shown to transport the nucleobases uracil, adenine and guanine with high affinities after heterologous expression in *E. coli* UraA mutants [48]. The localization of PLUTO exclusively in the plastid envelope was demonstrated by transient expression of corresponding GFP-fusion proteins in *Arabidopsis* leaf protoplasts. So far, PLUTO represents the only known nucleobase transport system in an organellar membrane.

The NCS2 protein family, also known as nucleobase ascorbate transporter (NAT) family is evolutionary widespread and present in prokaryotes, fungi, protists, plants and mammals [14]. Most characterized NCS2 proteins were shown to transport xanthine, uric acid and uracil (Fig. S1) with the exception of the human homologs like hSVCT1 and hSVCT2 that do not transport nucleobases but L-ascorbate instead [14]. Ten NCS2 members are present in *E. coli*, among these the uracil transporter UraA [28], the xanthine permeases XanQ and XanP [20], and the adenine permease PurP [3]. As an NCS2 member in plants, Maize leaf permease 1 (Lpe1) was identified in mutants with defects in chloroplast development and membrane integrity. However, no experimental evidence exists about the subcellular localization of Lpe1 [38].

Expression of *Arabidopsis* members from the NAT clade of NCS2 proteins have been characterized in great detail. Based on a multiple sequence alignment, the NAT proteins are split into five clades (I–V) [30]. Accordingly, AtNAT1–AtNAT3 belong to clade I, AtNAT4, AtNAT9 and AtNAT10 are part of clade II, AtNAT5–AtNAT8 are part of clade III, and AtNAT11 and AtNAT12 belong to clade V of NAT proteins [30].

* Corresponding author at: Universität Kaiserslautern, Pflanzenphysiologie, Postfach 3049, D-67653 Kaiserslautern, Germany. Tel.: +49 631 205 2505; fax: +49 631 205 2600.
E-mail address: moehlmann@biologie.uni-kl.de (T. Möhlmann).

http://dx.doi.org/10.1016/j.bbamem.2014.08.013
0005-2736/

The allocation into different clades correlates with their expression during the life cycle of *Arabidopsis*. Some of the members of this gene family show ubiquitous expression (*AtNAT12*), while the expression of other *AtNAT* genes is restricted to specific tissues (*AtNAT7*, *AtNAT8*, *AtNAT9*). In addition, most *AtNATs* show pronounced expression in vascular tissues, indicating that the encoded proteins might have a function in long-distance transport of metabolites [30]. All analyzed mutant lines of AtNAT family members including several double- and triple mutants belonging to the same clade lack obvious phenotypical differences compared to the wild type. These observations might be due to a high redundancy of NAT functions in *Arabidopsis*. Either the functions can be compensated by other NAT proteins or by nucleobase transporters of different protein families.

First structural information on NAT proteins came from the *E. coli* uracil/H^+ symporter UraA crystal structure in complex with uracil. UraA consists of 14 transmembrane segments (TMs) which are divided into two inverted repeats (TM1–TM7 and TM8–TM14) and a pair of antiparallel β-strands with an important role in structural organization and substrate recognition located between TM3 and TM10 [28]. Furthermore, the structure is arranged in two domains, a core and a gate domain. While the core domain seems to be important for substrate selectivity and proton/sodium translocation, conformational changes of the gate domain result in an alternating access mechanism of substrate transport [28].

Besides the NCS families, other transporters mediate nucleobase uptake in *Arabidopsis*. The AzgA proteins define a group of membrane proteins which are distantly related to the NAT (NCS2) family with homologs in plants, fungi, bacteria and archaea [4]. AzgA-like proteins are named after AzgA from *Aspergillus nidulans* encoding a proton-symporter specific for hypoxanthine, guanine and adenine. Two proteins, with significant similarity to AzgA, namely AtAzg1 and AtAzg2, have also been identified in *Arabidopsis thaliana*. These proteins share 36.5% and 38.5% identical amino acids with AzgA, respectively [29]. Homozygous mutant lines of the allele *AtAzg1-1* and *AtAzg1-2* showed increased resistance on 8-azaguanine and 8-azaadenine compared to the wildtype and this effect was even more pronounced in *AtAzg1* and *AtAzg2* double mutants indicating that AtAzg proteins are of high importance for adenine and guanine uptake into *Arabidopsis* cells.

In plants two additional protein families with nucleobases as typical substrates exist. These are the purine permeases (PUP) and ureide permeases (UPS). Substrates of PUP proteins are adenine, cytosine and the cytokinins kinetin and trans-zeatin [2,15]. Recently, pyridoxine (Vit B6) was identified as additional substrate [41]. Substrates of UPS proteins are uracil and allantoin [5,10,33,37].

For the NAT proteins in *Arabidopsis*, the substrates have not been identified for any member of this large family of transport proteins despite various attempts to express them in well-established eukaryotic systems [30]. Furthermore, structural information about these plant NCS2 proteins is lacking.

Therefore, the aim of this work was to first identify the biochemical properties of selected NAT proteins from *Arabidopsis*, namely AtNAT3 and AtNAT12. The expression of the corresponding genes in *E. coli UraA* mutants allowed for a detailed biochemical characterization. Second, the structure–function relationship of AtNAT12 was analyzed. Using UraA from *E. coli* as a template, a validated three-dimensional homology model of AtNAT12 was constructed. Based on the homology model, docking studies and mutational analyses, critical residues involved in substrate binding have been identified to gain insight into NAT transport function.

2. Material and methods

2.1. Strains and media

For the biochemical characterization of NAT3 and NAT12 and the analysis of NAT12 mutants, an *E. coli* transposon insertion strain lacking the endogenous uracil permease UraA JD23420 obtained from the National Institute of Genetics (Shizuoka, Japan, http://www.shigen.nig.ac.jp/ecoli/strain/top/top.jsp) was used. Cells were grown at 37 °C in YT medium consisting of 0.5% yeast extract, 0.8% peptone, 0.25% NaCl, pH 7.0 with or without ampicillin (200 mg l^{-1}) and kanamycin (25 mg l^{-1}). *E. coli* XL1Blue cells (Stratagene) were used for the propagation of plasmids and grown at 37 °C in YT medium containing ampicillin (200 mg l^{-1}) and tetracycline (10 mg l^{-1}).

2.2. Heterologous expression of NAT3 and NAT12 in E. coli JD23420

For the heterologous expression in *E. coli* JD23420, the full-length coding region of NAT3 and NAT12 was amplified with Pfu polymerase from *Arabidopsis* leaf cDNA using the primers NAT3pTACMAT2_fwd (XhoI restriction site) and NAT3pTACMAT2_rev (KpnI restriction site) or NAT12pTACMAT2_fwd (XhoI restriction site) and NAT12pTACMAT2_rev (KpnI restriction site), respectively (for primers see Table S1). The PCR product was cloned into the cleaved vector pTAC-MAT-Tag2 (Sigma Aldrich). The NAT3 and NAT12 constructs were transformed in *E. coli* JD23420 cells and cells were grown in YT medium containing ampicillin and kanamycin. At an OD_{600} value of 0.5, the NAT expression was initiated by the addition of isopropyl β-D-1-thiogalactopyranosid (IPTG) with a final concentration of 0.02%. The cells were grown for 2 h and harvested by centrifugation for 5 min at 4500 *g* at 4 °C. The cell pellets were resuspended with potassium phosphate buffer (50 mM, pH 7.0) to an OD_{600} value of 5 and stored on ice until use for the uptake experiments.

2.3. Site directed mutagenesis

For the generation of NAT12 mutants, the construct pTACMAT-Tag2::NAT12 was used as a template for site-directed mutagenesis which was carried out with QuikChange II Site-Directed Mutagenesis Kit (Agilent Technologies) according to the manufacturer's instructions. Primers used for mutagenesis were listed in Table S1.

2.4. Uptake experiments with radiolabelled substrates

Uptake with radiolabelled nucleobases [^{14}C]-uracil, [^{14}C]-guanine or [^{14}C]-adenine (10^{12}Bq mol^{-1}) were performed as described in Witz et al. [48]. For the time-dependent uptake of substrates, nucleobases were added with a final concentration of 20 μM. To test the effect of different concentrations of the uncoupler carbonylcyanide m-chlorophenylhydrazone (CCCP), this substance was added to the uptake medium containing 20 μM radiolabelled uracil. For the competition studies, competitors were added at ten-fold excess (200 μM) to the uptake medium containing 20 μM radiolabelled nucleobases. The analyses of NAT12 mutants were carried out with nucleobase concentrations corresponding to the half of K_M-values (for adenine 0.87 μM, for guanine 1.22 μM and for uracil 14.92 μM). The incubation time was 2 min for the determination of the apparent K_M-values, the competition studies and the CCCP-study and 5 min for the analysis of NAT12 mutants.

2.5. Generation of GFP fusion constructs and transient expression studies in Arabidopsis leaf protoplasts

For transient expression studies in *Arabidopsis* leaf protoplasts, *NAT3* and *NAT12* full-length coding regions were amplified from *Arabidopsis* leaf cDNA with Pfu polymerase and the primers NAT3pGFP2_fwd and NAT3pGFP2_rev or NAT12pGFP2_fwd and NAT12pGFP2_rev, respectively (for primer sequences see Table S1). The corresponding PCR products were cloned into the multiple cloning site of pGFP2 upstream of the GFP coding region [22]. Isolated *Arabidopsis* leaf protoplasts were transformed with column-purified plasmid DNA as described in Yoo et al. [52]. After an incubation for 24 h at 22 °C in the dark the protoplasts were analyzed with a Leica TCS SP5II microscope (GFP: 488 nm

excitation and 505 to 540 nm detection of emission through a 63 × 1.2 water immersion objective, chlorophyll autofluorescence: 488 nm excitation and 649 to 770 nm emission wavelength). The data were analyzed using Leica confocal software.

2.6. Construction of the sequence alignment

Multiple alignments of protein sequences of NCS2 members were performed with ClustalW [42]. The accession numbers of the NCS2 proteins used for the sequence alignment are listed in the legend of Fig. S1.

2.7. Homology modeling

The three-dimensional model of NAT12 was built using the crystal structure of UraA in complex with uracil in the inward-open conformation (PDB ID 3QE7) as a template. Homology modeling was achieved using the HHPred server [40]. The corresponding NAT12 model was selected based on the E-value ($E = 10^{-55}$) and p-value ($p = 3.2 \times 10^{-60}$) and the three-dimensional model was created using Modeller [35] as this software is associated with the HHPred server. For a better visualization, the prolonged N-terminus that did not align with UraA, residues 1–168, was removed. Quality control analysis of the model using a Ramachandran plot [27] identified over 90% residues in the favoured region. Only 3.2% of the residues were in the outlier region of the Ramachandran plot.

2.8. Molecular docking

For the molecular docking analysis with the identified substrates of NAT12, namely adenine, guanine and uracil, the NAT12 model and the ligands were prepared using Autodock Tools 1.5.6 [36]. After the preparation and choosing the search space, the substrates were docked into the NAT12 structure using Autodock vina [44]. The best binding pose for each substrate was selected with respect to total energy and experimental knowledge.

2.9. Plant material and growth conditions

For the analysis of *NAT3* and *NAT12* transcript levels, rosettes of wildtype and transgenic *A. thaliana* (L.) Heynh. 4-week old plants

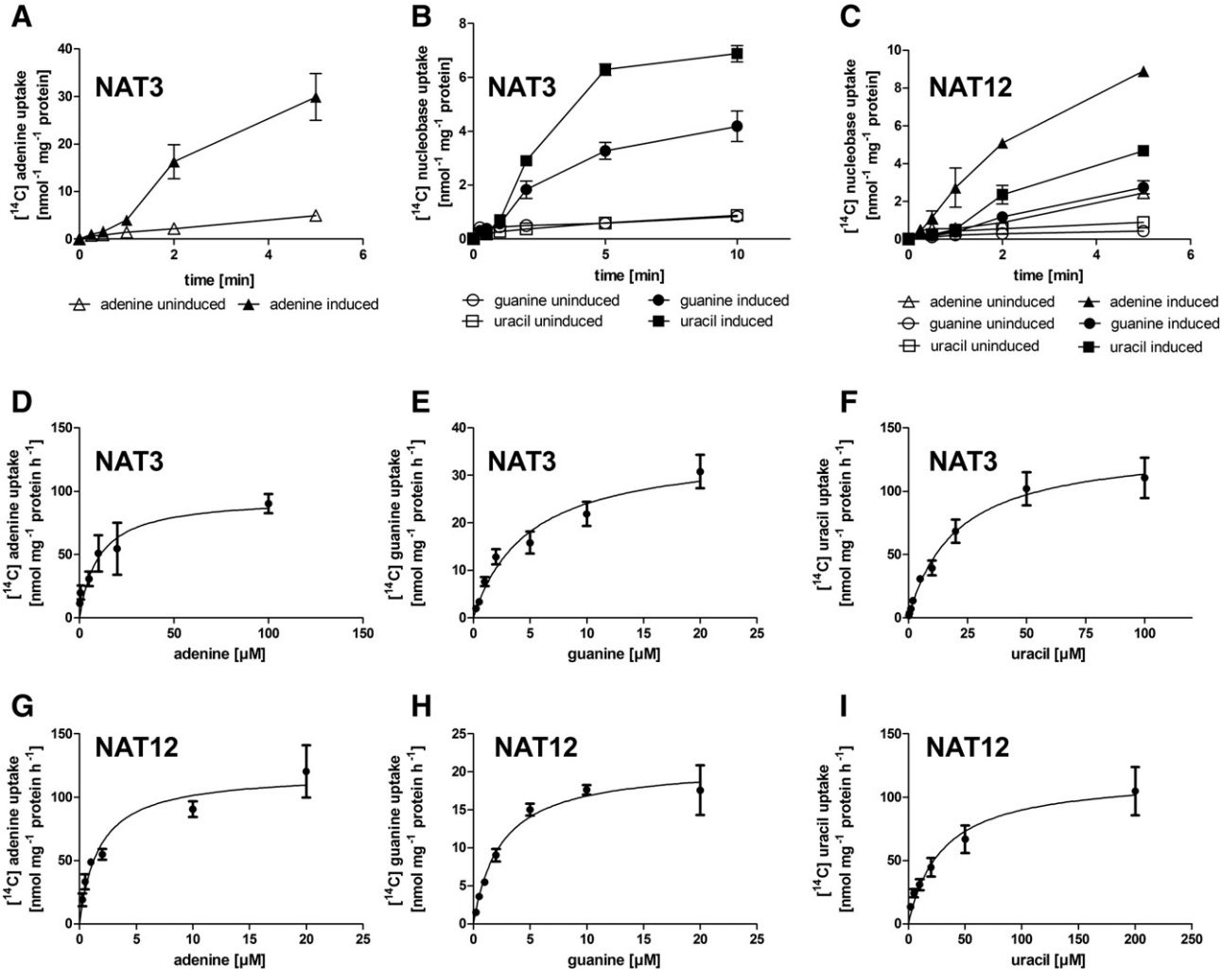

Fig. 1. Time courses and concentration dependencies of [^{14}C]-adenine, -guanine and -uracil uptake by NAT3 and NAT12 heterologously expressed in *E. coli* UraA KO mutants. (A,B) Time courses of adenine (A), guanine and uracil (B) uptake with a substrate concentration of 20 μM by NAT3 expressed in *E. coli* cells. Filled symbols represent the mean ± SE of IPTG-induced cells expressing NAT3, empty symbols represent the mean ± SE of uninduced cells used as a control. (C) Time course of adenine, guanine and uracil uptake with a substrate concentration of 20 μM by NAT12 expressed in *E. coli* cells. Filled symbols represent the mean ± SE of nucleobase uptake by IPTG-induced cells expressing NAT12, empty symbols represent the mean ± SE of nucleobase uptake by uninduced cells used as a control. (D,E,F) concentration dependence of adenine (D), guanine (E) and uracil (F) uptake by NAT3 expressed in *E. coli* cells. Uptake of [^{14}C]- nucleobases was measured for 2 min. (G, H, I), concentration dependence of adenine (G), guanine (H) and uracil (I) uptake by NAT12 expressed in *E. coli* cells. Uptake of [^{14}C]- nucleobases was measured for 2 min. Data shown in all subfigures A-I represent the mean of at least three independent experiments ± SE, with three replicates per individual experiment.

were used. Prior to germination, seeds were incubated for one day in the dark at 4 °C for imbibition in standardized ED73 soil [46]. Plant growth was carried out at 22 °C and 120 μmol quanta m^{-2} s^{-1} in a 10 h light/14 h dark regime.

2.10. Quantitative RT-PCR

Quantitative RT-PCR (qRT-PCR) was performed as given in Leroch et al. [26]. Gene specific primers used are listed in Table S1. The gene *At1g07930* encoding elongation factor 1α (EF1α) was used for quantitative normalization [7].

3. Results & discussion

3.1. Biochemical characterization of AtNAT3 and AtNAT12

To date, no plant NAT family member has been functionally characterized, except for Lpe1 from maize [1]. Extensive effort has been undertaken to analyze the biochemical characteristics by heterologous expression of *Arabidopsis* NAT proteins in various eukaryotic systems [30]. As we were able to express the distantly related NCS1 protein PLUTO in *E. coli* cells [48], we aimed to use this system for NAT proteins from *Arabidopsis*. For this we chose NAT3 and NAT12, showing high expression in *Arabidopsis* and belonging to different clades [30]. Both proteins were cloned in suitable expression vectors and expression was induced in *E. coli* mutants lacking the bacterial endogenous uracil permease UraA, obtained from the National Institute of Genetics, Shizuoka, Japan.

After induction of NAT expression, *E. coli* cells showed uptake of [^{14}C]-uracil, [^{14}C]-adenine and [^{14}C]-guanine in a time dependent manner (Fig. 1). In general, adenine showed higher uptake than uracil and guanine. Adenine uptake in NAT3 expressing cells was linear with time for at least 2 min and accounted for 16.3 μmol mg^{-1} protein, whereas uninduced cells imported only 2.2 μmol mg^{-1} protein, by this induced cells exceeded adenine transport by a factor of eight (Fig. 1A). The time course of nucleobase uptake for all other substrates in NAT3 and NAT12 expressing cells showed similar time linearity for at least 2 min. The difference between induced and uninduced cells at the 2 min time point was at least fourfold. Substrate dependent uptake of all nucleobases tested followed Michaelis–Menten kinetics. The apparent affinities (K_M) of NAT3 mediated nucleobase transport were 10.12 μM for adenine, 4.85 μM for guanine and 19.95 μM for uracil (Fig. 1D–F). The corresponding affinities for NAT12 mediated transport are 1.74 μM (adenine), 2.44 μM (guanine) and 29.83 μM (uracil) (Fig. 1G–I). Thus, both proteins exhibit higher affinities for the purine nucleobases compared to uracil and NAT12 exhibits higher affinities to purine nucleobases compared to NAT3.

All characterized mammalian nucleobase transporters of the NCS2 family, except for rSNBT1, transport only L-ascorbic acid whereas non-mammalian and non-plant NCS2 members either transport purines or pyrimidines. The only NCS2 protein of higher eukaryotes which is known to transport purine and pyrimidine nucleobases is *Rattus norvegicus* rSNBT1 [50] which is in addition the closest relative from higher eukaryotes to NAT12 [14], (Fig. S1). Therefore, the relationship between plant and non-primate mammalian proteins is reflected by the substrate spectrum of the corresponding proteins. We will come back to this point when discussing structure–function aspects of NAT proteins.

To address the question whether L-ascorbate might be a further substrate of NAT3 or NAT12 competition studies were performed with all substrates. However, no significant reduction of nucleobase transport, measured at concentrations of 20 μM, was detected by adding a tenfold higher amount of L-ascorbate (Fig. 2). In addition L-ascorbate was added to growing *E. coli* cells and the intracellular concentration was measured enzymatically after incubation for 120 min. No differences between NAT expressing cells to controls were observed (data not shown). Therefore, our results clearly indicate that L-ascorbate is no substrate for NAT3 or NAT12. This result is in accordance with previous findings showing that *Arabidopsis* NAT mutants were shown to not affect ascorbate levels [30]. In addition Lpe1 from maize was heterologously expressed in *A. nidulans* and used for competition experiments with L-ascorbate. It was concluded that ascorbate binds to Lpe1 but is not transported [1].

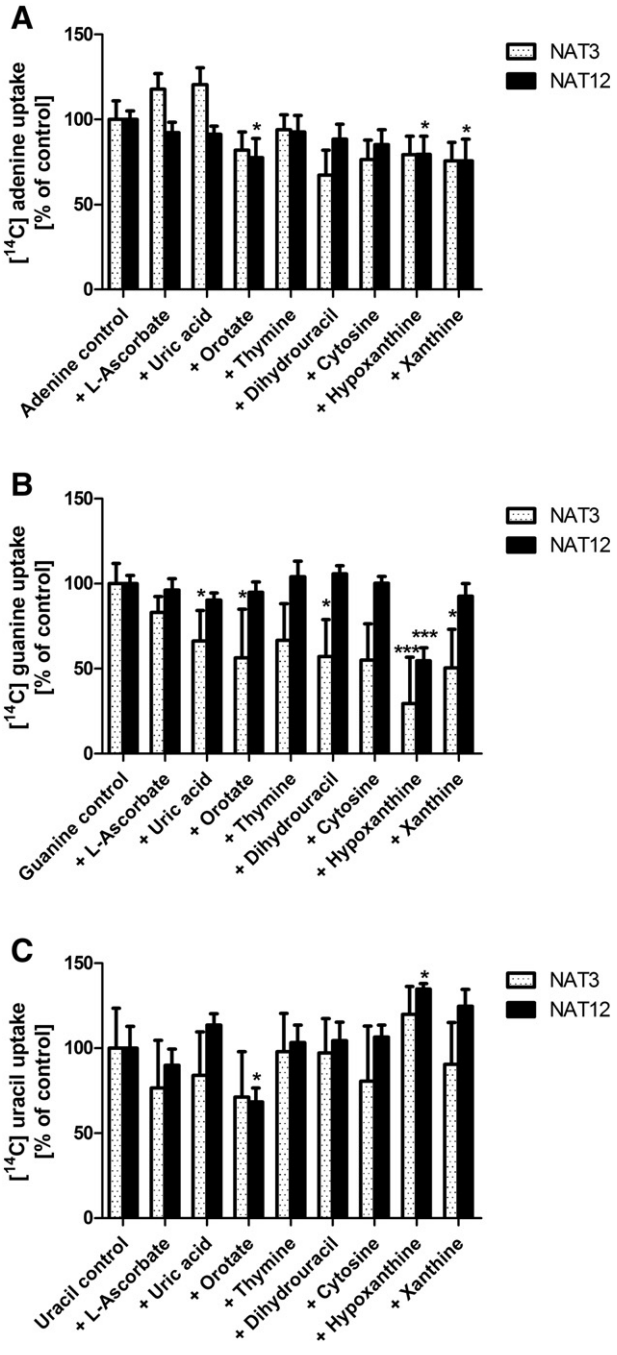

Fig. 2. Competition studies with NAT3 and NAT12 heterologously expressed in *E. coli*. Direct uptake studies with [^{14}C]-adenine (A), [^{14}C]-guanine (B) and [^{14}C]-uracil (C) were performed after heterologous NAT3 (spotted bars) and NAT12 (black bars) expression in *E. coli* UraA KO cells lacking the endogenous uracil importer. The uptake was measured with nucleobase concentrations of 20 μM and several competitors were added at 10-fold excess (200 μM). The data represent the mean of net uptake rates of at least three independent experiments (±SE). The asterisks indicate differences compared to the control based on Student's *t*-test (* = $p < 0.05$; *** = $p < 0.005$).

Competition studies further indicated that other compounds structurally related to nucleobases might be further substrates of NATs.

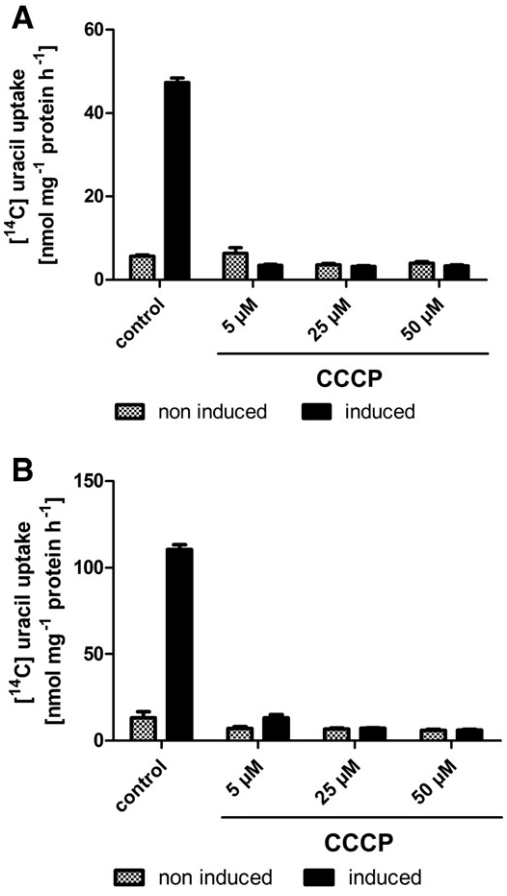

Fig. 3. The effect of the protonophore CCCP on NAT3 and NAT12 mediated uracil uptake. The effect of the protonophore CCCP was measured on [^{14}C]-uracil uptake by NAT3 (A) and NAT12 (B) heterologously expressed in *E. coli* UraA KO-mutants (black bars). Checked bars represent the uptake into uninduced cells used as controls. The uptake was measured with a uracil concentration of 20 µM and CCCP was added with rising concentrations of 5, 25 and 50 µM. The data represent the mean of at least three independent experiments ± SE.

We tested uptake of all three radiolabelled substrates (20 µM each) in NAT3 and NAT12 expressing cells for competition with structural analogs given at tenfold excess (Fig. 2). Guanine uptake facilitated by NAT3 was markedly reduced to about 30% in the presence of hypoxanthine (Fig. 2B). All other tested substrates were less effective, allowing no conclusion on relevance as a substrate. A similar picture became apparent when potential effectors were tested for an influence on NAT12 mediated nucleobase transport. Only hypoxanthine reduced guanine uptake to 55% of control values with high significance ($p < 0.005$, Fig. 2B).

Among the NCS2 transporters from higher eukaryotes, rSNBT1 was shown to transport hypoxanthine in addition to other purines and uracil [14,50]. Whether hypoxanthine is in fact a further substrate of NAT proteins and if functional similarities to rSNBT1 proteins can be related to structural similarities has to be tested in future studies.

By use of the proton uncoupler carbonylcyanid-m-chlorophenylhydrazone (CCCP) a clear inhibition of [^{14}C]-uracil transport was observed (Fig. 3). CCCP inhibited uracil transport mediated by NAT3 completely (Fig. 3A) and a similar effect was observed for NAT12 (Fig. 3B) at the relatively low concentration of 5 µM. Most likely, NAT3 and NAT12 function as nucleobase–proton symporters. This is similar to UraA, XanQ, UapA and UapC where a proton coupled mode of transport has already been demonstrated [14,16,28].

3.2. Subcellular localization

Both NAT3 and NAT12 were predicted with high probability to have a plastidic subcellular localization [39]. Therefore, we analyzed the subcellular localization of NAT-GFP fusion proteins after heterologous expression in *Arabidopsis* and Tobacco leaf protoplasts. Remarkably, both, NAT3 and NAT12 fusion proteins clearly did not colocalize with the chloroplast autofluorescence (Figs. 4 and S2). Both fusion proteins were located to structures resembling the plasma membrane. Similar results were previously obtained for a NAT12 fusion protein expressed in *Arabidopsis* cell culture [30]. In addition, results obtained from the *Arabidopsis* subcellular database (SUBA) confirm a localization in the plasma membrane based on several proteome studies [17].

Interestingly, compared to other NCS2 family members, NAT12 exhibits a distinct prolonged N-terminus of about 150 amino acids. To

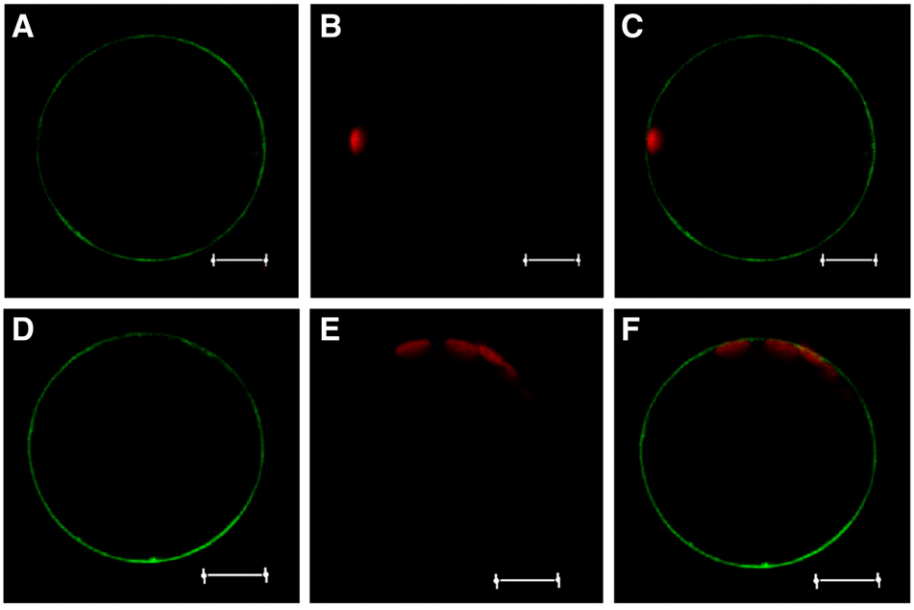

Fig. 4. Localization of NAT3- and NAT12-GFP-fusion constructs transiently expressed in *Arabidopsis* leaf protoplasts. To further investigate the subcellular localization of NAT3 (A–C) and NAT12 (D–F), transient expression studies of both proteins were performed with NAT-GFP fusion proteins in *Arabidopsis* leaf protoplasts. (A,D) NAT-GFP fluorescence; (B,E) chlorophyll-autofluorescence; (C,F) merge. The scale bars represent a size of 10 µm.

exclude a translation in the transient system from three other putative start codons within the N-terminus, all three corresponding methionines were mutated to alanines, thus allowing for only full length NAT12 synthesis. However, the mutated protein showed a similar subcellular localization as described before (Fig. S2).

To date, PLUTO remains the only nucleobase transporter described to be localized in the inner envelope membrane of plastids [48]. By the above experiments we add NAT3 and NAT12 to the many other nucleobase transporters shown or predicted to be located to the plasma membrane. Examples of others are the ureide permeases GmUPS1-1 and GmUPS1-2 from soy bean which are targeted to the plasma membrane [5], and also *Arabidopsis* AtUPS 1 and 2 are predicted to be localized to the secretory pathway [37,39]. In addition, there is experimental evidence for a localization in the plasma membrane of at least two other NAT proteins, namely AtNAT7 and 8 [30]. Also for the purine permease AtPUP1 a localization in the plasma membrane was confirmed with YFP-studies [41]. The apparently high redundancy of these transport systems complicates the clear adjudication of physiological function to individual proteins although NAT12 was shown to be quite highly and constitutively expressed based on microarray data and the analysis of Promoter–GUS fusion proteins [30,53]. However, an obvious phenotype of NAT mutants is lacking [30].

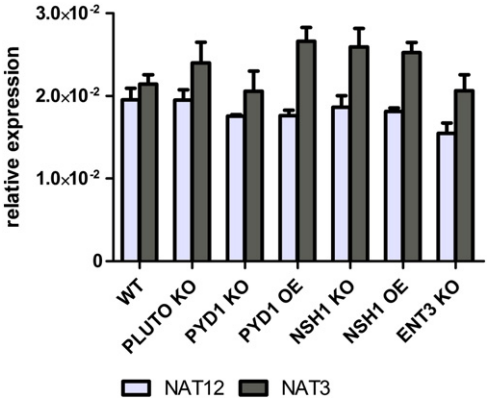

Fig. 5. Relative *NAT3* and *NAT12* expression in 4-week old *Arabidopsis* rosette leaves using quantitative RT-PCR. The transcript level of NAT3 and NAT12 was analyzed in different *Arabidopsis* mutants compared to the wildtype in relation to the reference gene *ef1α*. Data represent the mean of three independent experiments ± SE. *PLUTO* = plastidic nucleobase transporter (At5g03555) [31]; *PYD1* = pyrimidine degradation enzyme 1 (At3g17810) [6]; *NSH1* = Nucleoside hydrolase 1 [54] (At2g36310); *ENT3* = Equilibrative nucleoside transporter 3 (At4g05120), [43]. Data were analyzed according to the Student's *t*-test with p-values >0.05 for all mutants.

3.3. Expression studies

Quantitative RT-PCR studies have been carried out to reveal changes in expression of NAT3 and NAT12 in *Arabidopsis* mutants of genes we have shown to be important for nucleotide metabolism. These are knockout plants of the plastidic nucleobase transporter PLUTO [31], knockout and overexpressor plants of the pyrimidine degradation enzyme 1 (PYD1) [6], knockout and overexpressor plants of the nucleoside hydrolase 1 [19] and knockout plants of the nucleoside transporter ENT3 [43]. The expression of NAT3 and NAT12 relative to the housekeeping gene ef1α in the mutant plants was compared to the expression in the wildtype but no significant change was observed (Fig. 5). The calculated significance p-value was above 0.05 in all cases (Fig. 5) indicating that the transcriptional regulation of these transporters in the analyzed plants seems to be of minor importance.

3.4. Structure–function relationship of AtNAT12

3.4.1. Sequence analysis

After the biochemical characterization of both NAT proteins we looked for structural characteristics of NAT3 and NAT12 in comparison to other NCS2 family members. Therefore, we first analyzed a corresponding alignment. The *Arabidopsis* NAT3 and 12 sequences were compared to the uracil transporter UraA from *E. coli* [28], xanthine transporters XanP [20] and XanQ [21] from *E. coli,* uric acid/xanthine transporters UapA and UapC from *A. nidulans* (Fig. 6) and the uracil permease PyrP from *Bacillus subtilis* [45]. *Arabidopsis* NAT proteins 11 and 12 show an N-terminal extension which does not align to the other NCS2 proteins (Figs. 6 and S3). Since we have eliminated the possibility of a role in subcellular targeting, future efforts will focus on the role of this N-terminal domain to clarify its function. As NAT12 is not regulated at the transcript level, a possible regulatory function of the N-terminus by posttranslational modifications such as phosphorylation may be possible. Based on protein phosphorylation site databases like PhosPhAt 4.0 [12,18], several phosphorylation sites with experimental evidence from phosphoproteome data were predicted for residues Ser-40, Thr-43, Thr-44, Thr-46, Ser-48 and Ser-50 in NAT12 [12,18]. The corresponding positions are marked with "P" in Fig. 6. Therefore it can be speculated about a regulatory function by a phosphorylation of the N-terminus which might regulate the nucleobase transport function of NAT12. This will be validated in future experiments.

NAT3 (clade I) and NAT12 (clade V) share 25% identical and 42% similar amino acids. The similarity between *Arabidopsis* NAT proteins and the uracil permease UraA from *E. coli* is about 35% (without the N-terminus not aligning to the UraA sequence) and there are highly conserved motifs present in all aligned protein sequences (Fig. S3). Among these are the so called QH-motif in transmembrane segment 1 (TM1) and the characteristic NAT-signature motif [Q/E/P]-N-X-G-X-X-X-X-T-[R/K/G] (red box, Figs. 6 and S3) which is a common feature of all NAT proteins [11].

3.4.2. NAT12 homology model

For further insights into structure–function relationships of NAT12, a homology model of NAT12 was created based on the structural information of UraA from *E. coli*. The sequence homology between NAT12 and UraA (15.3% sequence identity and 34.5% sequence similarity), without considering the prolonged N-terminus of NAT12 which does not align to UraA, is sufficient to obtain a suitable structure of NAT12 [42]. Homology modeling was performed using HHPred server [40] and Modeller software [35]. The quality of the best model was checked with Ramachandran plot [27] which identified over 90% residues of the model in the favoured region of the plot. Only 3.2% of the residues were in the outlier region of the Ramachandran plot.

The NAT12 structural model is composed of 14 TM segments and divided into two inverted repeats of TM1–TM7 and TM8–TM14 related to each other around an axis parallel to the membrane bilayer (Fig. 7). This feature is very common among a number of transporters [51] and also apparent in NCS2 member UraA from *E. coli* [28], NCS1 proteins Mhp1 from *Microbacterium liquefaciens* [47] and PLUTO from *A. thaliana* [49]. In the middle of the NAT12 structure, two antiparallel β-strands are located between TM3 and TM10, similar to UraA, where an important role in structural organization and substrate recognition was assumed [28]. Moreover, the 14 transmembrane helices of NAT12 are arranged in a core domain consisting of TM1-4 and TM8-9 and the

Fig. 6. Alignment of NAT3 and NAT12 with other NCS2-type protein sequences from different organisms. NCS2 proteins from *Arabidopsis thaliana* NAT3 (At2g26510) and NAT12 (At2g27810), *Escherichia coli* UraA (P0AGM7), XanP (P0AGM9) and XanQ (P67444), *Aspergillus nidulans* UapA (Q07307) and UapC (P48777) and *Bacillus subtilis* PyrP (YP_003865951) protein sequences were aligned using ClustalW (www.ebi.ac.uk). The residues are shown according to their conservation mode (highly conserved residues in black). NAT12-residues marked with asterisks were mutated in the course of this work. Residues with green asterisks are involved in NAT12 substrate binding. Amino acids marked with a blue "P" represent putative phosphorylation sites of NAT12 based on PhosPhAt analysis. The QH-motif and the NAT-signature motif are marked with red boxes.

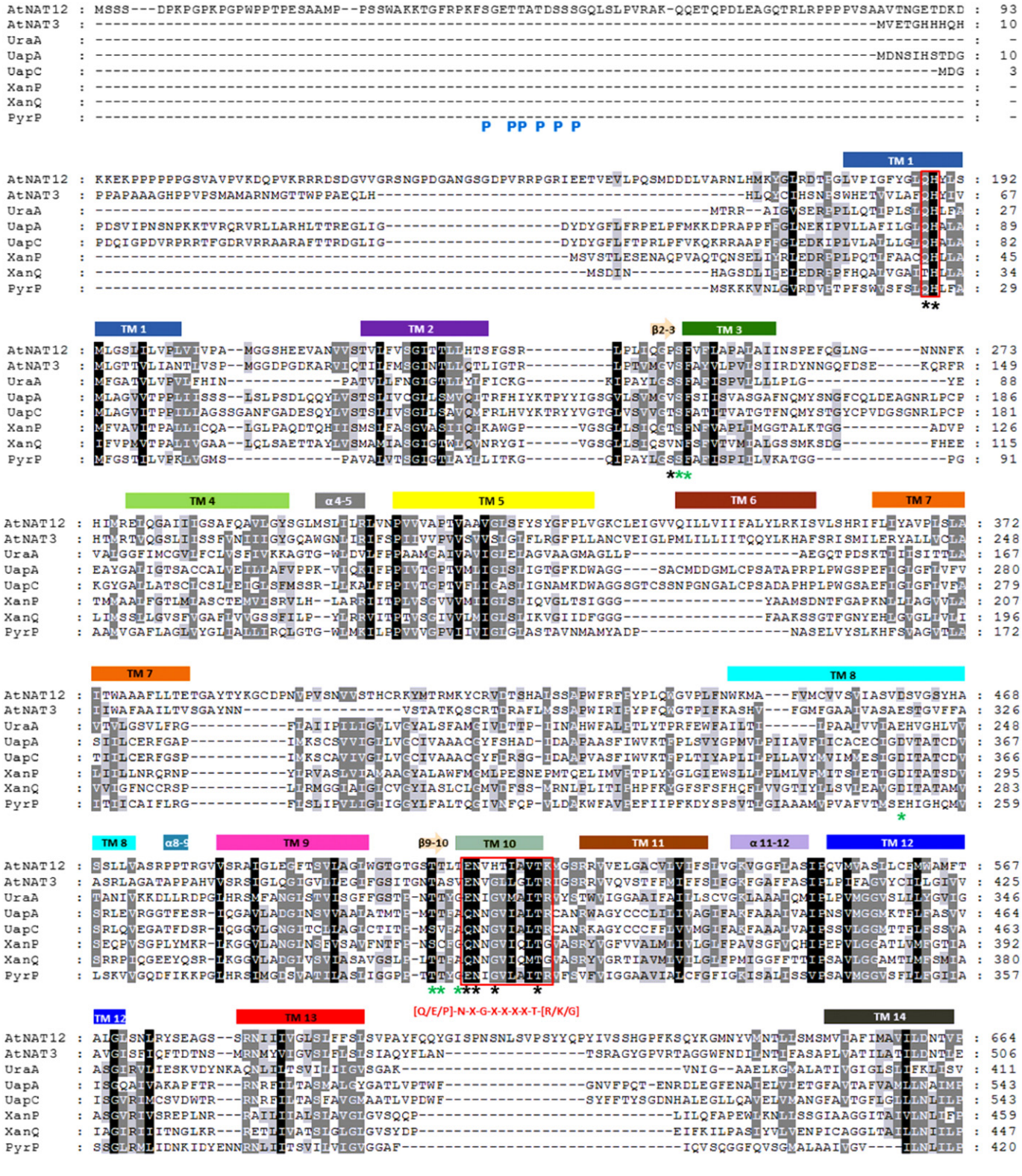
TM 1
TM 2
β2-3
TM 3
TM 4
α 4-5
TM 5
TM 6
TM 7
TM 8
α8-9
TM 9
β9-10
TM 10
TM 11
α 11-12
TM 12
TM 13
TM 14
[Q/E/P]-N-X-G-X-X-X-X-T-[R/K/G]

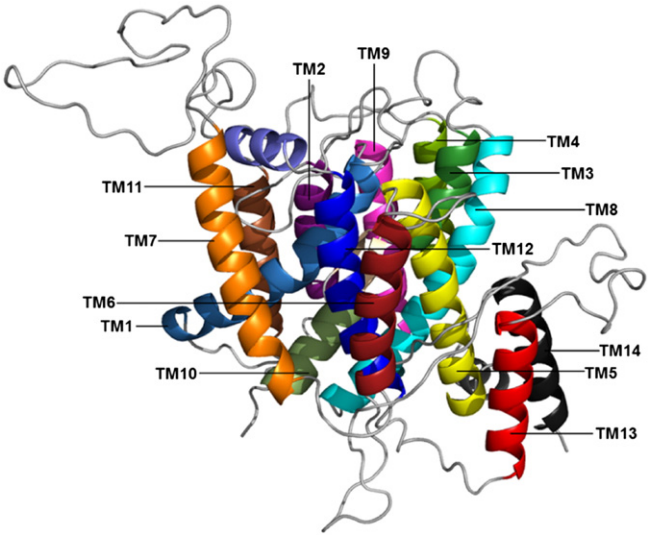

Fig. 7. NAT12 homology model with marked TMs. A three-dimensional model of NAT12, residues 169–671, was built using HHPred server and Modeller based on structural information of UraA. The TMs are marked in colors according to the alignment in Fig. 6. In the model, the prolonged N-terminus and a part of the longer C-terminus were removed for a better visualization.

gate domain consisting of TM5-7 and TM10-14 (Figs. 7 and 8A) indicating a similar function to UraA; where the core domain provides the molecular basis of substrate selectivity and proton translocation, while gate domain conformational changes allow for the transport of the substrate [28]. The substrate binding site of NAT12 is located in the center between the core and the gate domain and in close proximity to the antiparallel β-strands (Fig. 8).

3.4.3. Docking studies

For a better understanding of the molecular mechanisms of substrate binding, adenine, guanine and uracil were docked into the catalytic pocket of NAT12 using Autodock vina [44] after the preparation of the ligands using Autodock Tools [36]. All three substrates bind into a shelter between the core and the gate domain of the protein and in close proximity to the antiparallel β-strands and the connecting loops of TM3 and TM10 (Fig. 8) as it is also the case for uracil in UraA [28]. In the binding pocket, the residues exhibit direct contacts with residues from TM3 (Phe-248), TM8 (Asp-461), the β-strands (Pro-246, Thr-507) or the small loop regions between the β-strands and TM3 or TM10 (Thr-508, Ser-247), respectively. Residues in these regions were also important for uracil binding in UraA [28] and UapA [23]. Furthermore, this protein region is highly conserved among NCS2 proteins (Figs. 6 and S3).

Uracil binds into the catalytic center of NAT12 with a hydrogen bond between pyrimidine N3 and residue Asp-461, two H-bonds between Ser-247 and pyrimidine N1 and the keto group at position 4, respectively, and a hydrogen bond with Thr-507 (Fig. 8C). Guanine interacts with NAT12 through two H-bonds between purine N7 and the two residues Ser-247 and Phe-248, respectively. Moreover, there are H-bonds present between the purine amino group at position 2 and Thr-508 and between purine N1 and Thr-507 (Fig. 8D). Adenine interactions are stabilized by four H-bonds between purine N3 and Phe-248 as well as Ser-247. Further H-bonds are present between purine N9 and Thr-507 and between purine amino group at position 6 and Asp-461 (Fig. 8E). The differences in guanine binding compared to adenine and uracil with respect to Asp-461 (interacting with adenine and uracil) and Thr-508 (interacting with guanine) might explain why hypoxanthine inhibits guanine uptake but not uptake of the other two substrates with a high significance value of $p < 0.005$ (Fig. 2).

3.4.4. Mutational analysis

NAT12 mutants of the corresponding residues were subsequently tested for their transport function of adenine, guanine and uracil after the expression in *E. coli* UraA knockout cells (Fig. 9). Furthermore, the presence of the protein in isolated membrane fractions of *E. coli* cells expressing the NAT12 mutants was validated using an anti-MAT-Tag-antibody (Fig. S4). Phe-248 aligns to Phe-155 in UapA and Phe-73 in UraA, respectively (Fig. 6). In both proteins, the phenylalanine is important for substrate binding. In UapA, Phe-155 represents one residue from the centrally located major substrate binding site and shows interactions between the backbone carbonyl of Phe-155 and either N9 of Xan7H or N7 of Xan9H [23]. Interestingly, Phe-155 can be functionally replaced by other residues in UapA [23]. In UraA, the two oxygen atoms of uracil form hydrogen bonds with the amide nitrogen atoms of Phe-73. Moreover, uracil is coordinated by van der Waals interactions involving Phe-73. The residue is also supposed to block access to uracil from the periplasm [28]. In NAT12 F248A mutants, adenine transport is significantly reduced to 36%, and this effect is even more pronounced for guanine and uracil, where the transport was reduced to 14% and 19% compared to control cells (Fig. 9), indicating an important role in substrate transport also in NAT12. In addition, the presence of aromatic residues around the substrates is also apparent in other transport proteins like UraA [28] and vSGLT [13]. Mutation of Asp-461 to an alanine leads to a significantly decreased transport of all three substrates. Adenine, guanine and uracil transport were reduced to 59%, 46% and 45% compared to the control, respectively (Fig. 9). These results are also in good agreement with the docking results where Asp-461 plays an important role in uracil and adenine binding. Furthermore, the corresponding residue Glu-241 in UraA binds uracil with two H-bonds and uracil transport was completely abolished when it was exchanged to an alanine [28]. Another important aspect is the fact that the translocation of protons in UraA relies on the protonation and deprotonation of several residues, among these Glu-241 [28]. Therefore, it might be possible that Asp-461 in NAT12 might also participate in proton translocation explaining the effects of mutation D461A on the transport of all substrates. The corresponding residue in UapA is also an Aspartate (Asp-360), which was also shown to effect the transport capacity of this protein [23]. Interestingly, all other NCS2 proteins with known substrate specificity possess a glutamate at the corresponding position except for NAT12 and NAT11 where an aspartate is present (Fig. S3).

Based on the NAT12 docking analysis, Ser-247 was shown to contribute to the binding of all three substrates. Indeed, the functional studies with mutant S247A indicated that adenine and guanine transport were completely abolished and uracil transport was significantly reduced to only 15% of the control (Fig. 9). These results confirmed a participation of this residue in substrate binding. Mutagenesis of the corresponding residue Ser-154 from UapA also had effects on substrate transport, depending on the substitution [23].

In NAT12, similar results were also obtained for the analysis of mutant P246A, affecting residue Pro-246, here adenine and guanine transport were completely abolished and this holds true also for uracil transport, which was very severely decreased (Fig. 9). This indicates an important role for the function of NAT12 depending on this residue. In addition, it is in close proximity to Ser-247 and also part of a β-strand, meaning that a substitution to an alanine might avoid a proper protein folding and function.

Thr-507 is another residue which was identified via docking studies and shown to participate in the binding of all three substrates. The complete loss of function in mutant T507A for all substrates confirmed this assumption (Fig. 9). When residue Thr-508 was exchanged to an alanine, guanine and uracil transport were completely abolished and also adenine transport was only 8% of the control (Fig. 9), although docking studies only showed a direct interaction of this residue with guanine. Thr-508 is part of the flexible loop region between a β-strand and TM10 and a substitution of this residue might lead to a different

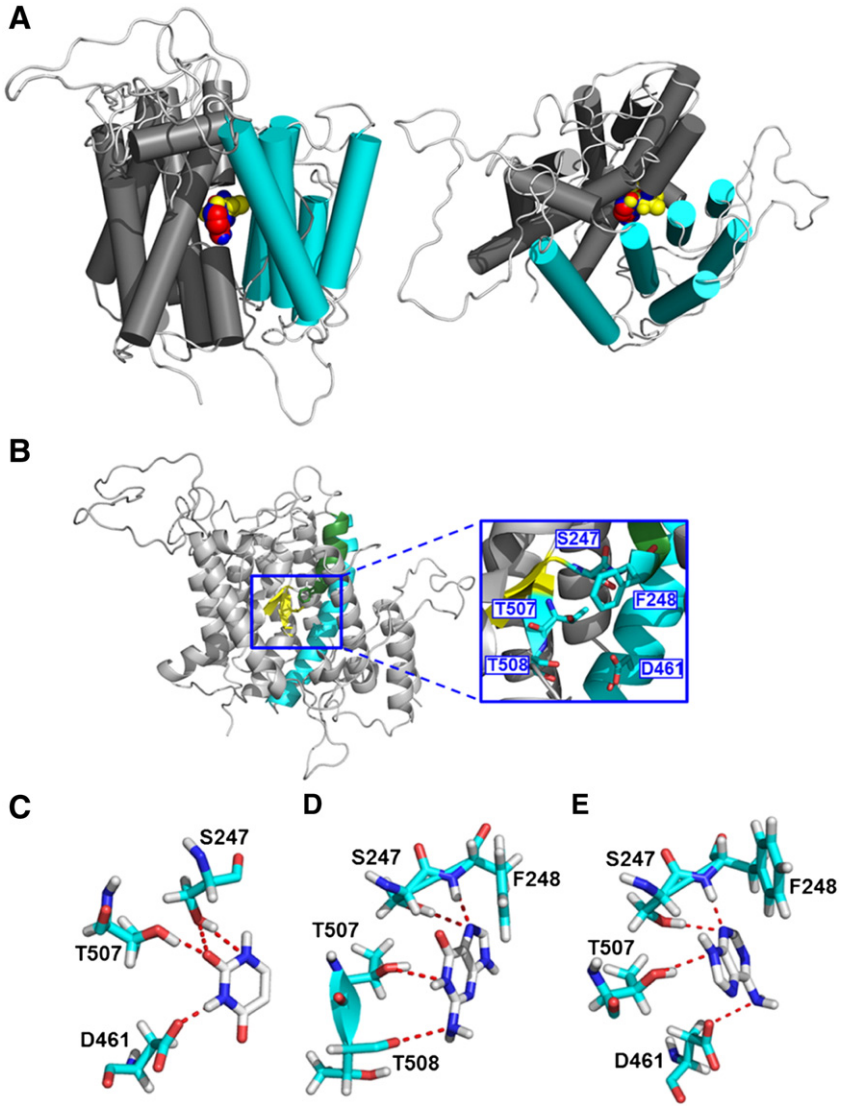

Fig. 8. Docking poses of substrates and position of residues involved in NAT12 substrate binding. (A) Schematic overview of the docking poses of the three substrates adenine (blue), guanine (yellow) and uracil (red). Uracil and adenine exhibit a very similar binding mode whereas guanine binding is slightly different. The core domain composed of TM1-4 and TM8-9 is colored in gray and the gate domain consisting of TM5-7 and TM10-14 is colored in cyan. (B) The NAT12 homology model with residues involved in substrate binding according to the docking analysis are marked in blue color. Transmembrane segments participating in binding are colored according to the colour scheme in Fig. 7: TM3 (darkgreen), TM8 (cyan) and the two antiparallel β-strands in the middle of the protein (yellow). (C,D,E) Docking poses of uracil (C), guanine (D) and adenine (E) based on Autodock vina results.

arrangement of this flexible binding site anticipating substrate transport. In general, the existence of the two discontinuous helices formed by two β-strands followed by unwound loop regions and two short α-helices is an unusual feature of transmembrane proteins and differentiates NAT proteins like UraA and also NAT12 from other integral membrane proteins [28].

Moreover, NAT proteins typically contain the NAT signature motif [24]. This motif [Q/E/P]-N-X-G-X-X-X-X-T-[R/K/G] is present in all sequences which were aligned (Figs. 6 and S3). From this we conclude that *Arabidopsis* NAT proteins are typical members of the evolutionary wide spread NAT/NCS2 family. NAT12 carries a His residue (His-514) instead of a glycine at position four of the motif (Figs. 6 and S3). Also *Arabidopsis* NAT11 and rice NAT 10 and 11 carry the His residue instead of a Gly at the respective position [30]. The position His-514 corresponding to Gly-411 in UapA and was identified as a residue of the substrate translocation pathway [23]. Mutation of His-514 in NAT12 lead to markedly reduced adenine, guanine and uracil transport, supporting the view of a similar important role of this position in NAT12. The first position of the NAT signature motif can either be a negatively charged glutamate (E), a polar glutamine (Q) or a small hydrophobic proline (P) and this position is part of the substrate binding site in UapA and UraA. Proline can be found in this position especially in the mammalian L-ascorbate transporters (Fig. S3) but not in the characterized nucleobase transporters of other organisms [24]. Xanthine or xanthine/uric acid transporters seem to possess a polar glutamine and uracil transporters like UraA, PyrP, rSNBT1 and also the NAT proteins exhibit a negatively charged glutamate except for NAT 9 (Fig. S3). As NAT3 and 12 both carry a glutamate (Glu-511) at the respective position, it is unlikely that L-ascorbate is substrate of these proteins. This view is in line with our observations on competition studies (Fig. 2) and a previous analysis of plant mutants [30]. Mutation of Glu-511 to an alanine in NAT12 affected purine base transport but not uracil (Fig. 9), further indicating an important function in substrate selectivity. However, the protein level in mutant E511A seems to be lower compared to the control (Fig. S4) and therefore it cannot be excluded that differences in the uptake behavior also result from slight differences in protein amount. Gln-408, corresponding to Glu-511 in NAT12 was identified as major substrate binding site in UapA accordingly [24]. At the same position, UraA carries a glutamate (Glu-290) important for uracil transport [28]. Purine or pyrimidine nucleobase

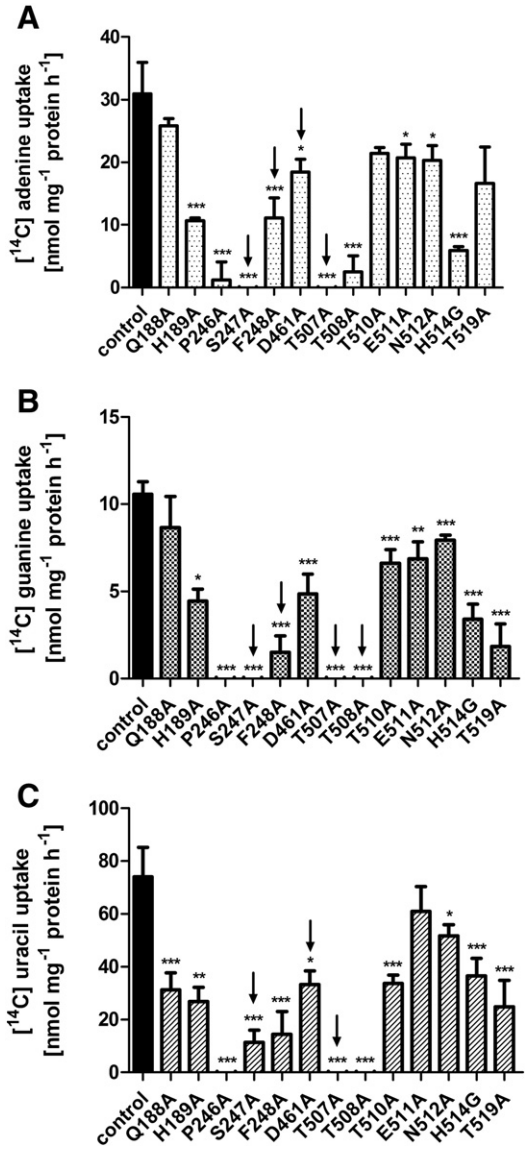

Fig. 9. Functional analyses of NAT12 mutants. Direct uptake studies with [^{14}C]-adenine (A), -guanine (B) and -uracil (C) were performed after heterologous NAT12 expression in *E. coli* cells lacking the endogenous uracil transporter UraA. Uptake was measured with nucleobase concentrations at half K_M-values of the substrates (0.87 μM adenine, 1.22 μM guanine, 14.92 μM uracil). The uptake data represent the mean of net uptake rates of at least three independent experiments ± SE. The asterisks indicate differences between NAT12 mutants and the control based on Student's *t*-test (* = $p < 0.05$; ** = $p < 0.01$; *** = $p < 0.005$). Black arrows mark residues involved in substrate binding based on docking experiments.

specific NAT proteins obviously rely stronger on substrate interaction at the Q/E position of the signature motif compared to the purine/pyrimidine nucleobase transporter NAT12 from higher eukaryotes, here plants.

At position two of the signature motif all characterized NAT proteins carry an asparagine (Asp-512 in NAT12), i.e. this position is highly conserved. In addition, Asp-409 is described as one of four invariant amino acids in UapA important for function [25], although exchange against residues of similar biochemical properties but different size did not result in changes in transport [24]. In NAT12 a small but significant reduction for the corresponding mutant (about 30%) was observed for all substrates (Fig. 9). This indicates an involvement in substrate transport, on the other hand this conserved residue is not of similar importance as in UapA. This is more like the corresponding residue in UraA where a similar degree of inhibition was observed as in NAT12 [28].

Ala-407 like Gln-408, positioned directly adjacent to the NAT-signature motif in UapA, is proposed to be part of the substrate binding site [24]. The corresponding Thr-510 in NAT12 was mutated to alanine and transport measurements showed significantly reduced transport of guanine and uracil (Fig. 9). Unfortunately, the protein amount in the mutant T510A seems to be lower compared to the control (Fig. S4) indicating that the reduced transport might be due to altered protein levels.

Thr-519 represents the penultimate residue of the NAT-signature motif in NAT12 and aligns to Thr-416 in UapA, where this residue is part of the cytoplasm facing substrate trajectory and seems to be involved in the stabilization of the protein tertiary intra-subdomain structure [23]. Furthermore, Thr-416 forms critical polar interactions with residue Gln-85 corresponding to Gln-188 in NAT12 [23]. In the NAT12 mutant T519A, adenine transport was reduced to 54% compared to control cells. Uracil and guanine transport were even decreased to 34% and 17% compared to non-mutated NAT12, respectively (Fig. 9). These results suggest that Thr-519 might also contribute to the substrate trajectory in NAT12.

Further amino acid positions outside the NAT signature motif were identified as part of the core domain. These are Gln-85/His-86 in UapA being parts of the so-called QH-motif [32] and corresponding to Gln-23/His-24 in UraA [28] and Gln-188/His-189 in NAT12 . The mutation of the conserved residue Gln-188 in NAT12 had no significant effect on adenine and guanine transport, but reduced uracil transport significantly to 42% of transport in control cells (Fig. 9). In contrast, mutation of residue His-189 to an alanine had obvious effects on the transport of all substrates indicating that the presence of the QH-motif seems to be important for a proper NAT12 transport function. The fact that the mutation relating to His-189 showed stronger effects on substrate transport might be due to the aromatic character of this amino acid which is often important for the surrounding of substrates during the transport process and which has been observed for several other membrane transporters [28]. In UapA, residues of the QH motif do not participate in substrate or ion binding. As polar charged residues in the middle of TMS1 they stabilize UapA in a way that is critical for trafficking (His-86) or for substrate transport catalysis (Gln-85) [32].

Supplementary data to this article can be found online at http://dx.doi.org/10.1016/j.bbamem.2014.08.013.

Acknowledgments

This work was supported by DFG-grant MO 1032/3-2 and IRTG 1830. We gratefully acknowledge the support of the work by Prof. H.E. Neuhaus and thank Pankaj Panwar for the advice and discussions concerning NAT12 modeling and docking. The authors declare that they have no conflict of interest.

References

[1] E. Argyrou, V. Sophianopoulou, N. Schultes, G. Diallinas, Functional characterization of a maize purine transporter by expression in *Aspergillus nidulans*, Plant Cell 13 (2001) 953–964.
[2] L. Bürkle, A. Cedzich, C. Dopke, H. Stransky, S. Okumoto, B. Gillissen, C. Kuhn, W.B. Frommer, Transport of cytokinins mediated by purine transporters of the PUP family expressed in phloem, hydathodes, and pollen of *Arabidopsis*, Plant J. 34 (2003) 13–26.
[3] K. Burton, Adenine transport in *Escherichia coli*, Proc. Biol. Sci. 255 (1994) 153–157.
[4] G. Cecchetto, S. Amillis, G. Diallinas, C. Scazzocchio, C. Drevet, The AzgA purine transporter of *Aspergillus nidulans*. Characterization of a protein belonging to a new phylogenetic cluster, J. Biol. Chem. 279 (2004) 3132–3141.
[5] R. Collier, M. Tegeder, Soybean ureide transporters play a critical role in nodule development, function and nitrogen export, Plant J. 72 (2012) 355–367.
[6] S. Cornelius, S. Witz, H. Rolletschek, T. Möhlmann, Pyrimidine degradation influences germination seedling growth and production of *Arabidopsis* seeds, J. Exp. Bot. 62 (2011) 5623–5632.
[7] C. Curie, T. Liboz, C. Bardet, E. Gander, C. Medale, M. Axelos, B. Lescure, Cis and trans-acting elements involved in the activation of *Arabidopsis thaliana* A1 gene encoding the translation elongation factor EF-1 alpha, Nucleic Acids Res. 19 (1991) 1305–1310.

[8] E. Cusa, N. Obradors, L. Baldoma, J. Badia, J. Aguilar, Genetic analysis of a chromosomal region containing genes required for assimilation of allantoin nitrogen and linked glyoxylate metabolism in *Escherichia coli*, J. Bacteriol. 181 (1999) 7479–7484.
[9] S. Danielsen, M. Kilstrup, K. Barilla, B. Jochimsen, J. Neuhard, Characterization of the *Escherichia coli* codBA operon encoding cytosine permease and cytosine deaminase, Mol. Microbiol. 6 (1992) 1335–1344.
[10] M. Desimone, E. Catoni, U. Ludewig, M. Hilpert, A. Schneider, R. Kunze, M. Tegeder, W.B. Frommer, K. Schumacher, A novel superfamily of transporters for allantoin and other oxo derivatives of nitrogen heterocyclic compounds in *Arabidopsis*, Plant Cell 14 (2002) 847–856.
[11] G. Diallinas, J. Valdez, V. Sophianopoulou, A. Rosa, C. Scazzocchio, Chimeric purine transporters of *Aspergillus nidulans* define a domain critical for function and specificity conserved in bacterial, plant and metazoan homologues, EMBO J. 17 (1998) 3827–3837.
[12] P. Durek, R. Schmidt, J.L. Heazlewood, A. Jones, D. Maclean, A. Nagel, B. Kersten, W.X. Schulze, PhosPhAt: the *Arabidopsis thaliana* phosphorylation site database. An update, Nucleic Acids Res. 38 (2010) D828–D834.
[13] S. Faham, A. Watanabe, G.M. Besserer, D. Cascio, A. Specht, B.A. Hirayama, E.M. Wright, J. Abramson, The crystal structure of a sodium galactose transporter reveals mechanistic insights into Na+/sugar symport, Science 321 (2008) 810–814.
[14] S. Frillingos, Insights to the evolution of Nucleobase-Ascorbate Transporters (NAT/NCS2 family) from the Cys-scanning analysis of xanthine permease XanQ, Int. J. Biochem. Mol. Biol. 3 (2012) 250–272.
[15] B. Gillissen, L. Bürkle, B. Andre, C. Kuhn, D. Rentsch, B. Brandl, W.B. Frommer, A new family of high-affinity transporters for adenine, cytosine, and purine derivatives in *Arabidopsis*, Plant Cell 12 (2000) 291–300.
[16] C. Gournas, I. Papageorgiou, G. Diallinas, The nucleobase-ascorbate transporter (NAT) family: genomics, evolution, structure–function relationships and physiological role, Mol. BioSyst. 4 (2008) 404–416.
[17] J.L. Heazlewood, R.E. Verboom, J. Tonti-Filippini, I. Small, A.H. Millar, SUBA: the *Arabidopsis* subcellular database, Nucleic Acids Res. 35 (2007) D213–D218.
[18] J.L. Heazlewood, P. Durek, J. Hummel, J. Selbig, W. Weckwerth, D. Walther, W.X. Schulze, PhosPhAt: a database of phosphorylation sites in *Arabidopsis thaliana* and a plant specific phosphorylation site predictor, Nucleic Acids Res. 36 (2008) D1015–D1021.
[19] B. Jung, C. Hoffmann, T. Möhlmann, *Arabidopsis* nucleoside hydrolases involved in intracellular and extracellular degradation of purines, Plant J. 65 (2011) 703–711.
[20] P. Karatza, S. Frillingos, Cloning and functional characterization of two bacterial members of the NAT/NCS2 family in *Escherichia coli*, Mol. Membr. Biol. 22 (2005) 251–261.
[21] E. Karena, S. Fillingos, The role of transmembrane segment TM3 in the Xanthine Permease XanQ of *Escherichia coli*, J. Biol. Chem. 286 (2011) 39595–39605.
[22] B. Kost, P. Spielhofer, N.H. Chua, A GFP-mouse talin fusion protein labels plant actin filaments in vivo and visualizes the actin cytoskeleton in growing pollen tubes, Plant J. 16 (1998) 393–401.
[23] V. Kosti, G. Lambrinidis, V. Myrianthopoulos, G. Diallinas, E. Mikros, Identification of the substrate recognition and transport pathway in a eukaryotic member of the nucleobase-ascorbate transporter (NAT) Family, PLoS One 7 (2012) e41939.
[24] M. Koukaki, A. Vlanti, S. Goudela, A. Pantazopoulou, H. Gioule, S. Tournaviti, G. Diallinas, The nucleobase-ascorbate transporter (NAT) signature motif in UapA defines the function of the purine translocation pathway, J. Mol. Biol. 350 (2005) 499–513.
[25] E. Krypotou, V. Kosti, S. Amillis, V. Myrianthopoulos, E. Mikros, G. Diallinas, Modeling, substrate docking, and mutational analysis identify residues essential for the function and specificity of a eukaryotic purine–cytosine NCS1 transporter, J. Biol. Chem. 287 (2012) 36792–36803.
[26] M. Leroch, S. Kirchberger, I. Haferkamp, M. Wahl, H.E. Neuhaus, J. Tjaden, Identification and characterization of a novel plastidic adenine nucleotide uniporter from Solanum tuberosum, J. Biol. Chem. 280 (2005) 17992–18000.
[27] S.C. Lovell, I.W. Davis, W.B. Arendall, P.I. de Bakker, J.M. Word, M.g Prisant, J.S. Richardson, D.C. Richardson, Structure validation by Calpha geometry: phi, psi and Cbeta deviation, Proteins 50 (2003) 437–450.
[28] F. Lu, S. Li, Y. Jiang, J. Jiang, H. Fan, G. Lu, D. Deng, S. Dang, X. Zhang, J. Wang, N. Yan, Structure and mechanism of the uracil transporter UraA, Nature 472 (2011) 243–246.
[29] T.A. Mansfield, N.P. Schultes, G.S. Mourad, AtAzg1 and AtAzg2 comprise a novel family of purine transporters in *Arabidopsis*, FEBS Lett. 583 (2009) 481–486.
[30] V.G. Maurino, E. Grube, J. Zielinski, A. Schild, K. Fischer, U.I. Flugge, Identification and expression analysis of twelve members of the nucleobase-ascorbate transporter (NAT) gene family in *Arabidopsis thaliana*, Plant Cell Physiol. 47 (2006) 1381–1393.
[31] G.S. Mourad, J. Tippmann-Crosby, K.A. Hunt, Y. Gicheru, K. Bade, T.A. Mansfield, N.P. Schultes, Genetic and molecular characterization reveals a unique nucleobase cation symporter 1 in *Arabidopsis*, FEBS Lett. 586 (2012) 1370–1378.
[32] A. Pantazopoulou, G. Diallinas, The first transmembrane segment (TMS1) of UapA contains determinants necessary for expression in the plasma membrane and purine transport, Mol. Membr. Biol. 23 (2006) 337–348.
[33] H.C. Pelissier, A. Frerich, M. Desimone, K. Schumacher, M. Tegeder, PvUPS1, an allantoin transporter in nodulated roots of French bean, Plant Physiol. 134 (2004) 664–675.
[34] M.H. Saier Jr., M.R. Yen, K. Noto, D.G. Tamang, C. Elkan, The transporter classification database: recent advances, Nucleic Acids Res. 37 (2009) D274–D278.
[35] A. Sali, T.L. Blundell, Comparative protein modelling by satisfaction of spatial restraints, J. Mol. Biol. 234 (1993) 779–815.
[36] M.F. Sanner, Python: a programming language for software integration and development, J. Mol. Graph. Model. 17 (1999) 57–61.
[37] A. Schmidt, Y.H. Su, R. Kunze, S. Warner, M. Hewitt, R.D. Slocum, U. Ludewig, W.B. Frommer, M. Desimone, UPS1 and UPS2 from *Arabidopsis* mediate high affinity transport of uracil and 5-fluorouracil, J. Biol. Chem. 279 (2004) 44817–44824.
[38] N.P. Schultes, T.P. Brutnell, A. Allen, S.L. Dellaporta, T. Nelson, J. Chen, Leaf permease1 gene of maize is required for chloroplast development, Plant Cell 8 (1996) 463–475.
[39] R. Schwacke, A. Schneider, E. van der Graaff, K. Fischer, E. Catoni, M. Desimone, W.B. Frommer, U.I. Flugge, R. Kunze, ARAMEMNON, a novel database for *Arabidopsis* integral membrane proteins, Plant Physiol. 131 (2003) 16–26.
[40] J. Söding, A. Biegert, A.N. Lupas, The HHpred interactive server for protein homology detection and structure prediction, Nucleic Acids Res. 33 (2005) W244–W248.
[41] N. Szydlowski, L. Bürkle, L. Pourcel, M. Moulin, J. Stolz, T.B. Fitzpatrick, Recycling of pyridoxine (vitamin B6) by PUP1 in *Arabidopsis*, Plant J. 75 (2013) 40–52.
[42] J.D. Thompson, D.G. Higgins, D.J. Gibson, CLUSTAL W: improving the sensitivity of progressive multiple sequence alignment through sequence weighting, position specific gap penalties and weight matrix choice, Nucleic Acids Res. 22 (1994) 4673–4680.
[43] M. Traub, M. Flörchinger, J. Piecuch, H.H. Kunz, A. Weise-Steinmetz, J.W. Deitmer, H.E. Neuhaus, T. Möhlmann, The fluorouridine insensitive 1 (fur1) mutant is defective in equilibrative nucleoside transporter 3 (ENT3), and thus represents an important pyrimidine nucleoside uptake system in *Arabidopsis thaliana*, Plant J. 49 (2007) 855–864.
[44] O. Trott, A.J. Olson, AutoDock Vina: improving the speed and accuracy of docking with a new scoring function, efficient optimization and multithreading, J. Comput. Chem. 31 (2010) 455–461.
[45] R.J. Turner, Y. Lu, R.L. Switzer, Regulation of the *Bacillus subtilis* pyrimidine biosynthetic (pyr) gene cluster by an autogenous transcriptional attenuation mechanism, J. Bacteriol. 176 (1994) 3708–3722.
[46] D. Weigel, J. Glazebrook, *Arabidopsis*. A Laboratory Manual, Cold Spring Harbor Laboratory Press, New York, 2002.
[47] S. Weyand, T. Shimamura, S. Yajima, S. Suzuki, O. Mirza, K. Krusong, E.P. Carpenter, N.G. Rutherford, J.M. Hadden, J. O'Reilly, P. Ma, M. Saidijam, S.G. Patching, R.J. Hope, H.T. Norbertczak, P.C.J. Roach, S. Iwata, P.J.F. Henderson, Structure and molecular mechanism of a nucleobase-cation-symport-1 family transporter, Science 322 (2008) 709–713.
[48] S. Witz, B. Jung, S. Fürst, T. Möhlmann, *De novo* pyrimidine nucleotide synthesis mainly occurs outside of plastids, but a previously undiscovered nucleobase importer provides substrates for the essential salvage pathway in *Arabidopsis*, Plant Cell 24 (2012) 1549–1559.
[49] S. Witz, P. Panwar, M. Schober, J. Deppe, F.A. Pasha, M.J. Lemieux, T. Möhlmann, Structure–function relationship of a plant NCS1 member — Homology modeling and mutagenesis identified residues critical for substrate specificity of PLUTO, a nucleobase transporter from *Arabidopsis*, PLoS ONE 9 (2014) e91343.
[50] S. Yamamoto, K. Inoue, T. Murata, S. Kamigaso, T. Yasujima, J.Y. Maeda, Y. Yoshida, K.Y. Ohta, H. Yuasa, Identification and functional characterization of the first nucleobase transporter in mammals: implication in the species difference in the intestinal absorption mechanism of nucleobases and their analogs between higher primates and other mammals, J. Biol. Chem. 285 (2010) 6522–6531.
[51] A. Yamashita, S.K. Singh, T. Kawate, Y. Jin, E. Gouaux, Crystal structure of a bacterial homologue of Na+/Cl-dependent neurotransmitter transporters, Nature 437 (2005) 215–223.
[52] S.D. Yoo, Y.H. Cho, J. Sheen, *Arabidopsis* mesophyll protoplasts: a versatile cell system for transient gene expression analysis, Nat. Protoc. 2 (2007) 1565–1572.
[53] P. Zimmermann, M. Hirsch-Hoffmann, L. Henning, W. Gruissem, Genevestigator. *Arabidopsis* microarray database and analysis toolbox, Plant Physiol. 136 (2004) 2621–2632.
[54] B. Jung, M. Flörchinger, H.-H. Kunz, M. Traub, R. Wartenberg, W. Jeblick, H.E. Neuhaus, T. Möhlmann, Uridine-Ribohydrolase (URH) is a key regulator of uridine degradation, Plant Cell 21 (2009) 876–891.